The importance of bubble ring-up and pulse length in estimating the bubble distribution from acoustic propagation measurements

S. D. Meers[1], T. G. Leighton[1], J. W. L. Clarke[1], G. J. Heald[2], H. A. Dumbrell[2], P. R. White[1]

[1] Institute of Sound and Vibration Research, University of Southampton, Highfield, Southampton, SO17 1BJ, UK. sdm@isvr.soton.ac.uk, tgl@isvr.soton.ac.uk, jwlc@isvr.soton.ac.uk, prw@isvr.soton.ac.uk
[2] Defence Evaluation and Research Agency, DERA Bincleaves, Newton Road, Weymouth, Dorset, DT4 8UR, UK. gjheald@dera.gov.uk, hadumbrell@dera.gov.uk

Abstract

Consideration is given to the effect of pulse length upon inverse methods of determining bubble population. Standard techniques of inversion are founded upon several basic assumptions. Consideration is given to these assumptions and the degree to which they may be compromised in oceanic measurements. This is demonstrated using experimental data taken during the recent Hurst Spit 2000 experiment. Finally a first illustration is made of how modelling of an oceanic bubble population may be used to add confidence to, and to infer extra information from, such bubble population measurements.

1. Introduction

A number of different techniques exist for bubble sizing including optical, electrochemical and acoustical. Acoustical techniques have been particularly successful owing to the fact that bubbles present a high impedance mismatch to acoustical energy. Methods of acoustic bubble sizing include the combination frequency technique [1, 2], the resonator system [3] and inversion of acoustic propagation [4-6]. This paper considers the latter technique, which can be used to determine bubble populations in general over a larger volume than the former, by making simple measurements of the characteristics of an acoustic disturbance propagating through a bubbly medium. Existing inversion techniques all rely on the same basic formulation and make similar assumptions, namely, that the bubble oscillates linearly in a free field and is driven by a plane wave. These assumptions allow linear bubble theory, as described by Commander and Prosperetti [7], to be applied to the problem.

The validity of such methods of determining bubble population must be carefully considered prior to any experimental measurements in order to ensure that any violations of the basic assumption stated above do not invalidate the results. This is of particular importance when considering measurements to be made in the surf zone as in the case of the recent experiment at Hurst Spit as discussed in Leighton *et al.* [8]. The length of pulse used in this environment is critical. Section 2 will investigate whether it is possible to select a pulse that ensures that linear, steady state bubble oscillation is achieved, but not so long that multi-paths and reverberation compromise the plane wave and free field assumptions.

Testing of the linear, steady state assumption is necessary because, owing to inertial effects, there is a finite the bubble 'ring-up' time (the interval from the start of motion of the bubble wall until it attains $1/e$ of the amplitude it would attain in steady state). Prior to reaching steady state oscillation the bubble response will be greatly reduced [9]. The nonlinear time-dependent response bubble of a bubble can be predicted from the formulations of [10] and Herring [11]:

$$\left(1-\frac{\dot{R}(t)}{c_0}\right)R(t)\ddot{R}(t)+\frac{3\dot{R}^2}{2}\left(1-\frac{\dot{R}(t)}{3c_0}\right)=\left(1+\frac{\dot{R}(t)}{c_0}\right)\frac{1}{\rho}\left\{p_B(t)-p_o-P\left(t-\frac{R(t)}{c_0}\right)\right\}+\frac{R(t)}{\rho c_0}\frac{dp_B(t)}{dt} \tag{1}$$

$$p_B(t)=\left(p_0+\frac{2\sigma}{R_0}\right)\left(\frac{R_0}{R}\right)^{3\kappa}-\frac{2\sigma}{R}-\frac{4\eta\dot{R}}{R} \tag{2}$$

Here R is the bubble wall radius, R_0 the equilibrium bubble radius, c_0 is the (constant) speed of sound in the liquid, ρ the density of the liquid, σ is the surface tension and η is the shear viscosity coefficient of the liquid. Also κ is the polytropic index of the gas within the bubble and p_0 is the hydrostatic pressure to which the bubble is subjected.

The existence of a ring-up time (which can readily be demonstrated by this model [9]) suggests that if the pulses are of short enough duration, the use of a steady state model could introduce additional errors into the inversion process, as it will not correctly predict the bubble response and thus its effect on the acoustic

TG Leighton, GJ Heald, HD Griffiths, G Griffiths, (eds.), 'Acoustical Oceanography', Proc. Institute of Acoustics Vol. 23 Part 2, 2001.

propagation. Section 3 will describe how this model may be used in a different fashion in order to infer extra information about an estimated bubble population.

2. Pulse length dependence of the inversion technique

As outlined in Section 1, in order to use standard techniques for inverting acoustic propagation characteristics to estimate the bubble population, a number of criteria must be met. They are that the bubble must oscillate linearly in a free field and be driven by a plane wave. This section will analyse some of the data obtained in the Hurst Spit experiment and then consider the validity of each one of the assumptions in that case.

2.1 Experimental Data

As part of the recent Hurst Spit trial, an experiment was designed whereby bubble size distributions would be estimated, via inversion technique, using pulses consisting of different numbers of cycles. For each frequency two pulses were emitted, firstly a 5 cycle pulse then a 20 cycle pulse. Each pulse was separated by 10 ms, hence the bubble population can be considered constant between pulses and the entire pulse train lasted just under 180 ms. The frequencies ranged between 200 kHz and 360 kHz in order to investigate the smaller range of bubble radii specified as objective (i) of Section 3 of Leighton *et al.* [8]. The experimental set-up is shown in Figure 1. Here the source and receiver were both positioned at Tx. Single frequency pulses were emitted and the backscattered reflection from a 50" diameter buoy measured. The source was positioned 2.35 metres from the buoy, 0.5 metres from the sea floor and at a depth of approximately 1 m. Associated details are given by Leighton *et al.* [8].

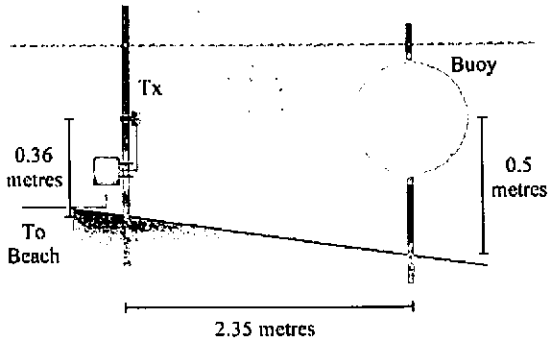

Figure 1. Experimental set-up, source and receiver positioned at Tx.

The attenuation caused by the presence of bubbles was measured by comparing experimental measurements to those made *in situ* under conditions of sustained calm and similar water depth where all other sensors [8] detected no measurable bubbles. Because this technique measures excess attenuation between bubble and bubble-free conditions, it is self-calibrated for any spherical spreading, absorption losses and the scattering function of the buoy itself.

Figure 2 shows the measured attenuation for both 5 and 20 cycle pulses and Figure 3 shows the resultant bubble populations calculated from these measurements.

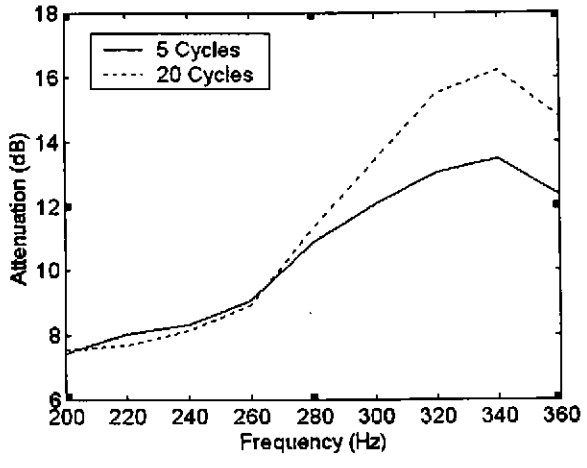

Figure 2. Measured attenuation for 5 and 20 cycle pulses. The pulse separation was 10 ms and the entire sweep of frequencies lasted 180 ms

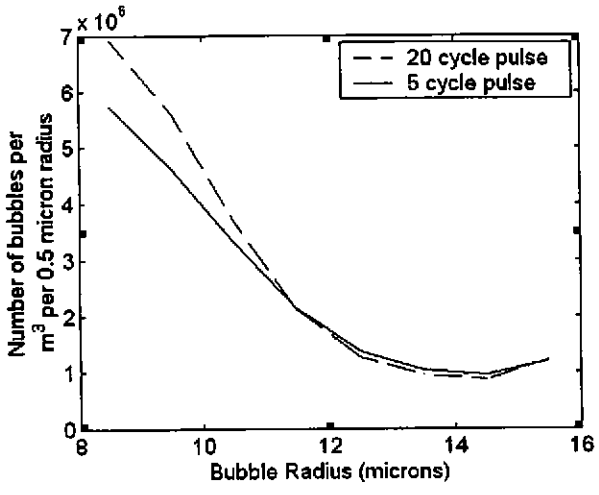

Figure 3. Estimated bubble populations for 5 and 20 cycles pulse. The measurement was made in a wind speed of 14-15 mph off shore breeze, with a water temperature of 11 °C and at a depth of ~1 m. The pH of the water was 6.12 and the dissolved oxygen content was 5.3 mg/litre. Estimation of bubble population was made by inversion of attenuation measurements following the method described in [4-6].

As can be seen from Figure 2 and Figure 3 the length of the insonification pulse affects the measured attenuation and, hence, the estimated bubble population. The difference in measured attenuation varies as a function of frequency and becomes small, <0.5 dB below 280 kHz. Unfortunately, owing to the statistical non-stationary characteristics of the system (i.e. in the surf zone bubble population is highly dependent upon wave breaking events), it has not been possible to quantify error bars for the data presented in Figures 2 and 3. However a similar trend was observed across a wide range of datasets. The assumptions inherent in the inversions used here will now be discussed.

2.2 Validation of Assumptions

2.2.1 Assumption 1: Plane Wave Propagation

In order for the plane wave condition to be met, the pulse must not suffer interference from either by multi-path reflections or in the limit, reverberation. Consideration is simplified if the bubble is in the far field of the source. The transition between near and far field for a plane transducer occurs at L^2/λ as discussed in [12], where L is the effective faceplate radius of the transducer and λ the wavelength of the radiated sound field. The source used in the Hurst Spit experiment had an effective faceplate radius of 50 mm. At 200 kHz this indicated that the transition to far field conditions occurred at 0.33 metres. Therefore the bubbles in over 93% of the direct beam path length are in the source's far field. However the presence of far field conditions does not guarantee planarity of the field which drive the bubbles into oscillation. The beam pattern of the source at 200 kHz is given in Figure 4. If a bubble is driven by multi-path reflections, these will reduce the validity of the plane wave assumption. Take, for example, the interference caused by reflection from the free surface. A first order estimate of the upper permissible bound of pulse length is determined by the difference in arrival times for both the direct path and the shortest non-direct path. Using the experimental set-up shown in Figure 1 the plane wave assumption is invalid for a pulse length greater than 110μs. Since the longest pulse duration used was 100 μs, the first non-direct reflection will arrive at the receiver after the duration of the direct pulse. Reflections from other entities (e.g. neighbouring bubbles) may reduce this upper limit.

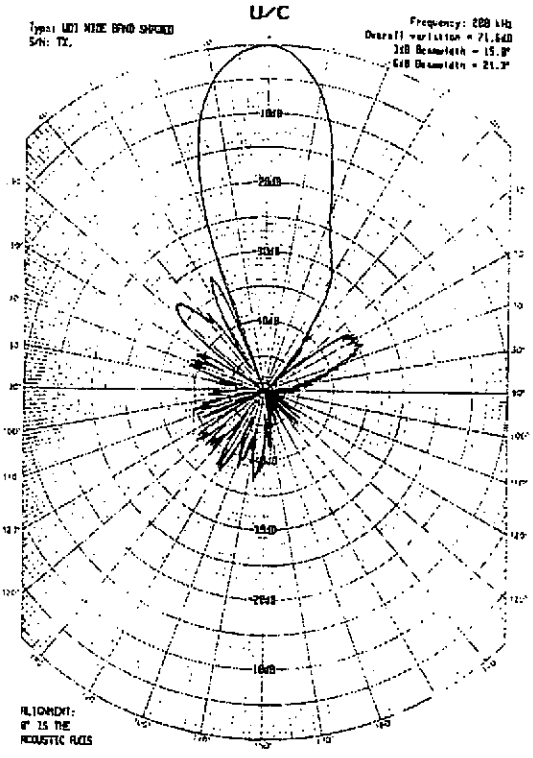

Figure 4. Beam Pattern at 200 kHz for source used in Hurst Spit sea trial: 3 dB beamwidth=15°; 6 dB beamwidth=21.3°.

2.2.2 Assumption 2: Free Field Conditions

Whilst the assumption of planarity relates to the field which drives the bubbles into pulsation, that that of free field conditions relates to the sound field emitted by those pulsations. This has two effects. First, if the bubble is not in free field, application of the free field assumptions which are ubiquitous in current oceanic bubble acoustics, can lead to errors: both the natural frequency and damping of bubbles in reverberant environments differ from the free-field values [13]. A bubble at a depth of 1 m will, for example, receive reverberation of its own emissions from the atmosphere/ocean surface just over 1 ms after it beings to emit. The 100 μs limit described above precludes this particular source of reverberation affecting the bubble's resonance characteristics [13], but it should be recalled that there are closer sources of reverberation (such as neighbouring bubbles). Second, since the emission from each bubble is finite in time (it rings up, may attain steady state, then rings down) then the reverberation from a bubble at a given range will affect the time-history of the pressure field at any point in the liquid. Two specific points of interest are at the receiver transducer (since from this the population is estimated, using a formulation which neglects reverberation), and at any given bubble (since the reverberant component will contribute, if only in a small way, to the driving field on the bubble).

2.2.3 Assumption 3: Linear Bubble Oscillation

As stated in Section 1 at the heart of the procedure for estimating bubble populations though inversion of propagation characteristics (attenuation and phase speed) is the assumption of linear, steady state bubble oscillations in the free field. However since these assumptions may be violated when short pulses of high amplitude are used, as may be the case in the surf zone, it is necessary to develop a model based on the non-linear time-dependent cross-section as described by Leighton *et al.* [8].

In the Hurst Spit experiment, attenuation along the ~4.7 m two-way direct propagation path was as much as 40 dB. Clearly propagation through the dense bubble populations which can be encountered in the surf zone may require high source amplitude (in this case a maximum of 28 kPa at the faceplate). Hence the degree to which bubble non-linearity can occur must be considered. For example, the solution of the Herring-Keller equation for an example bubble in the surf zone is illustrated in Figure 5. The rise time of the bubble can be clearly seen in Figure 5(a) and for this case it can be seen that steady state oscillations are not achieved within 20 cycles (see Figure 3 of Leighton *et al.* [8] for a discussion of some implications of this). Whilst any pulse contains more than a single frequency, Figure 5(b) clearly shows that a considerable amount of energy is invested in the harmonics. This, and the strong asymmetry in the expansion/collapse of Figure 5a, indicate that this bubble cannot be considered to be undergoing linear oscillations in these insonation conditions.

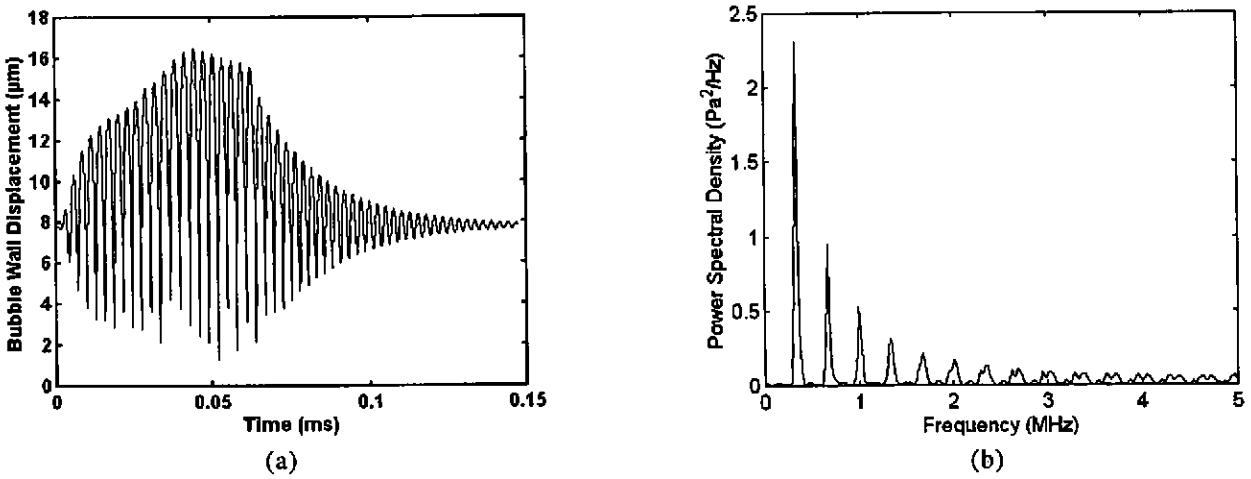

(a) (b)

Figure 5. (a) Solution of equation (1) for bubble wall displacement of a 7.8 μm bubble insonified by a 20 cycle pulse at 339 kHz at 28 kPa acoustic pressure amplitude; (b) Power Spectral Density of the radiated pressure from the bubble at a distance of 0.01 m.

Having established that linear, steady state oscillations are not occurring in the bubble cloud when insonified by short pulses for at least some of the propagation path, it is desirable to be able to quantify the effect this has. Figure 6 shows the results predicted by the non-linear, time-dependent and range-dependent forward model [8] for the bubble population estimated by the measurements made during the Hurst Spit experiment. It shows the predicted levels of attenuation, for insonification of the bubble population by pulses of duration 5, 20, 50 and 100 cycles. It demonstrates a pulse length dependence in the attenuation of the cloud. The small change in attenuation between the 50 and 100 cycle pulses suggest that the cloud has reached steady state for the 50 cycle pulse. The 20 cycles pulse shows a small drop in attenuation of the order 1 dB above approximately 300 kHz while the 5 cycles pulse shows stronger degradation in attenuation across the whole frequency range. As shown in Section 2.2.1, the planarity condition prohibits the use of pulses of duration longer than 100 μs i.e. 20 cycles at 200 kHz.

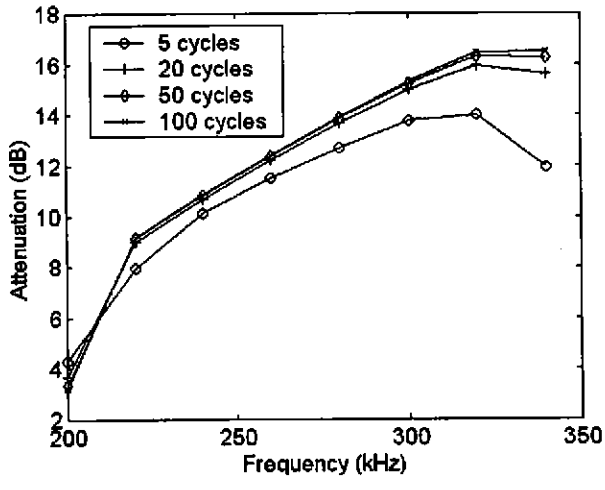

Figure 6. Theoretical calculations of attenuation for 5, 20, 50 and 100 cycle pulses based upon a bubble population estimated during the Hurst Spit experiment.

3. Extrapolation of bubble population

The data processed to date from the Hurst Spit experiment has concentrated on answering objective 1 from Section 3 of Leighton *et al.* [8] Hence the priority has been to invert the attenuation measurements to give the bubble population for an equilibrium bubble radius of between 9 μm and 15 μm. The only other measurements to such small bubble sizes given in Figure 6 were taken, not in the surf zone, but in oceanographically deep water (as explained in [1]). These were by Farmer and Vagle 1989 [14], and show a peak at $R_0 = 20$ microns. That such a peak exists, and is expected from oceanographic considerations, was confirmed Phelps and Leighton [1]. The evidence from the Hurst Spit 2000 data (Figure 3) suggests that such a peak does not seem to be present in that surf zone trial. This suggests that this population of small bubbles is newly entrained, and dissolution effects have not has sufficient time to reduce their number. This is reasonable given the conditions and video data.

Having satisfied objective 1 from [8], a more speculative test is undertaken. As can be seen from Figure 7, the Hurst Spit bubble population has a gradient similar to that of 'deep' water datasets and hence a hypothetical extrapolation of the bubble population may be made where the gradient of the surf zone population follows that of the deep water measurements ('Extrapolation 1'). The equation used for this first extrapolation is:

$$n_b = 3*10^{11} R_0^{-5} \tag{3}$$

where n_b is the number of bubbles per cubic metre per micrometer increment in radius.

However, as can also be seen from Figure 7, the Hurst Spit data points have an absolute level similar to that obtained for larger bubbles in the surf zone, as obtained by Leighton and the generation of student previous to those involved in the Hurst Spit 2000 trial [2, 15]. (A direct comparison for surf zone bubbles as small those of the Hurst Spit data is not possible, as no previous data exists – see objective (i) of Leighton *et al.* [8]). Hence it is not unreasonable to suggest and test Extrapolation 2, which intersect the Hurst Spit data and the previous surf zone data. Is it possible to use the time-dependent model to say whether Extrapolation 2, or Extrapolation 1 (which by contrast intersect the Hurst Spit data and the previous surf zone data), is a more likely fit to the surf zone population which provide the attenuation data at Hurst Spit? The two extrapolations are shown in Figure 7, the population of Extrapolation 2 being given by:

$$n_b = 6*10^6 \, e^{-0.02 R_0} \tag{4}$$

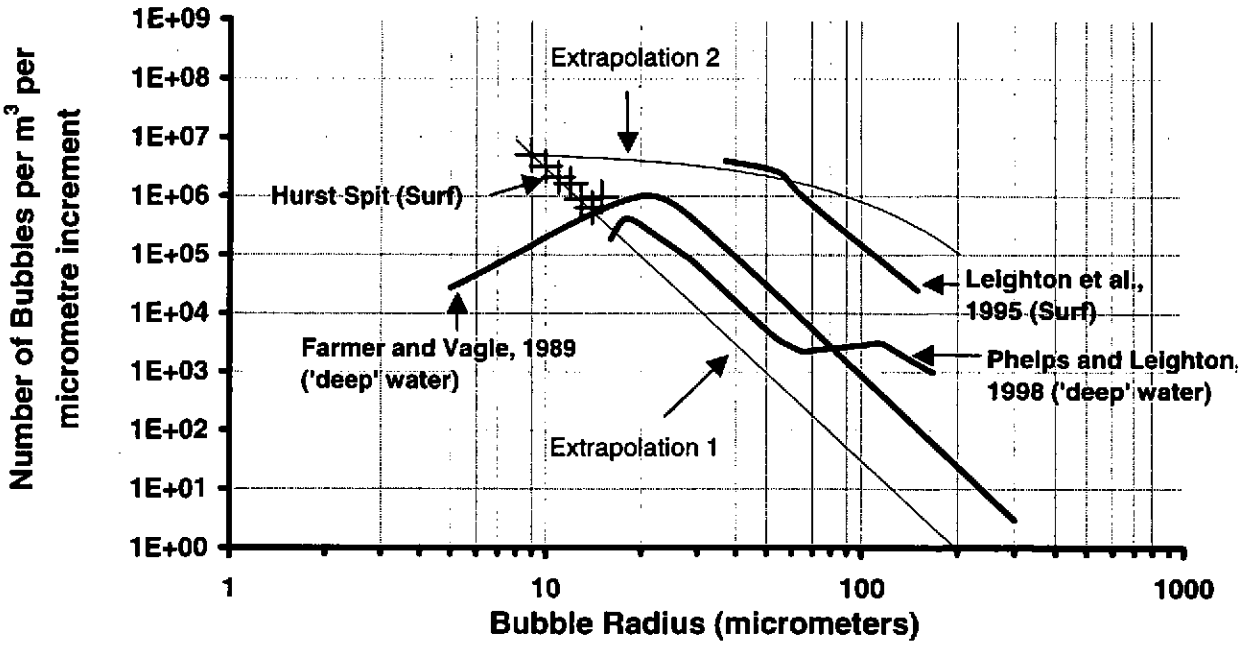

Figure 7. A comparison of several experimental measurements of bubble populations. Phelps and Leighton 1998 [1] and Farmer and Vagle 1989 [14] are two measurements of 'deep water' oceanic bubble population. A measurement of surf-zone bubble populations was taken by Leighton and the previous generation of students [2, 15] using the combination frequency technique. The population measurement marked Hurst Spit is the population measured during the sea trial by inversion. The crosses represent measured data points and the two thin lines are the two proposed extrapolations.

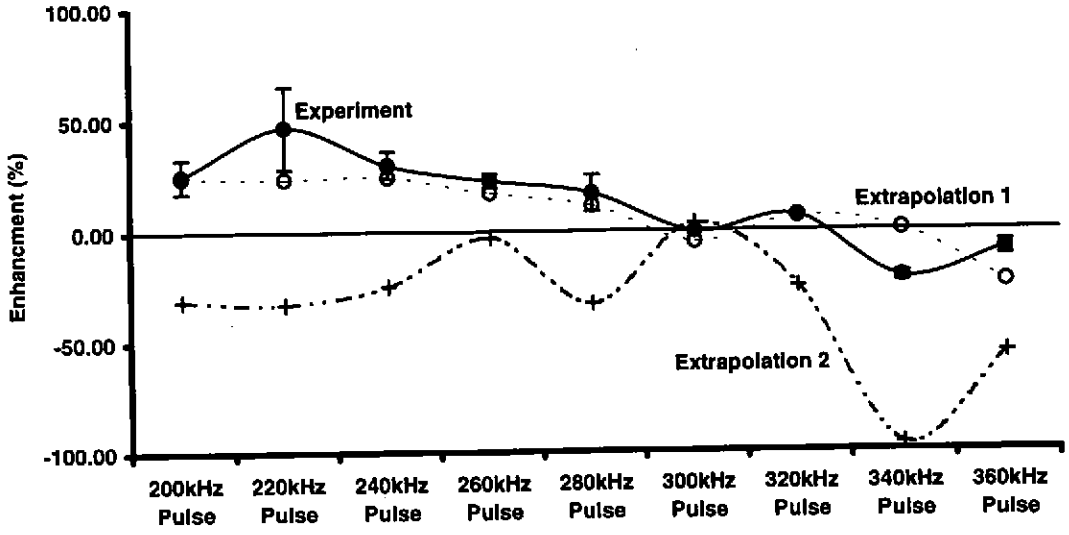

Figure 8. Experimental (solid line) and theoretical measurement (dashed lines) of the relative attenuation between short and long pulses. The error bars represent one standard deviation of the experimental results. Two sets of results for theoretical populations are shown. The first is Extrapolation 1 (Equation 3) of the Hurst Spit surf-zone population and the second is Extrapolation 2 (Equation 4).

This question can be answered by calculating from the model of [8] the differences in the levels of attenuation for 5 and 20 cycle pulses. The relative attenuations Extrapolations 1 and 2 are shown in Figure 8. It is apparent that the theoretical results for Extrapolation 1 show much better agreement with the experimental measurements than do those of Extrapolation 2.

It is important to note that the numbers of bubbles present were linearly scaled for the purposes of modelling the cloud so as to keep processing time within reasonable limits. However, because of the steep gradient of the extrapolated population the large bubbles, above ~50 μm in radius, are removed from the calculation. Thus the technique described above confirms the population distribution used up to a radius of 50 μm. Beyond this radius the model results confirm that the assumption, implicit in the scaling, that the contribution of bubbles greater than 50 μm is insignificant. This does not confirm the shape of the extrapolated population other than that the numbers of large bubbles must be small.

4. Conclusions

This paper has highlighted several considerations associated with estimation of bubble populations via inversion of acoustic propagation in the surf zone. The necessity of using short pulses in this environment to avoid interference with the acoustic propagation by multi-path reflections or reverberation casts a shadow of doubt over many of the basic assumptions made by the model of linear bubble oscillation used in standard inversion techniques. Comparison was made between modelled attenuation for a number of pulses containing different numbers of cycles. The discussion highlighted the problem that it was necessary to use more cycles to achieve linear oscillation than was possible without experiencing multi-path reflections. This problem will be exacerbated at lower frequencies when the pulse length necessary to contain a certain number of cycles (hence achieving steady-state oscillations) will be considerably longer. In the case where this circumstance makes use of the model by Commander and Prosperetti questionable, it may be possible to use a non-linear time-dependent equation of motion to describe the bubble response, and to invert propagation characteristic for bubble populations.

Objective (i) from Section 3 of Leighton *et al.* [17] has been accomplished, in that bubble population measurements were made in a critical size region where data for the surf zone was not previously available. The differences between this preliminary data and 'deep water' data in the same size range can be attributed to specific oceanographic features. In Section 3 it was shown how models of an extrapolated bubble population can be used to estimate the general trend of a bubble population, if measurements are only available over a limited range of bubble radii.

Acknowledgements

The authors would like to acknowledge the technical assistance of Rob Stainsbridge, Keith Sims, Dave Edwards Mark Bampton and particularly John Taylor and Tony Edgeley during the Hurst Spit trial. We are also very grateful to the New Forest District Council, particularly Matt Hosey, for allowing us access to the beach and EPSRC grant reference GR/M38094 for providing the funding to make this work possible.

References

[1] Phelps AD and Leighton TG. Oceanic Bubble Population Measurements using a buoy-deployed combination frequency technique. *IEEE J. Oceanic Eng*, 1998; **23**: 400-410.

[2] Phelps AD, Ramble DG, Leighton TG. The use of a combination frequency technique to measure the surf zone bubble population. *J. Acoust. Soc. Am.*, 1997; **101**: 1981-1989.

[3] Farmer DM and Vagle S. Bubble Measurements using a resonator system, in *Natural physical processes associated with sea surface sound.* T.G. Leighton (ed.) University of Southampton, UK, 155-162 (1997).

[4] Commander KW and McDonald RJ. Finite-element solution of the inverse problem in bubble swarm acoustics. *J. Acoust. Soc. Am.*, 1991; **89**: 592-597.

[5] Duraswami R, Prabhukumar S and Chahine GL. Bubble counting using an inverse acoustic scattering method. *J. Acoust. Soc. Am.*, 1998; **104**: 2699-2717.

[6] Terrill EJ, Lada G and Melville WK. Surf-Zone Bubble Populations, in *'Acoustical Oceanography', Proceedings of the Institute of Acoustics Vol. 23 Part 2, 2001,* T G Leighton, G J Heald , H Griffiths and G Griffiths, (eds.), Institute of Acoustics, (this volume), pp. 212-219.

[7] Commander KW and Prosperetti A. Linear pressure waves in bubbly liquids: Comparison between theory and experiments. *J. Acoust. Soc. Am.*, 1989; **85**: 732-746.

[8] Leighton TG, Meers SD, Simpson MD, Clarke JWL, Yim GT, Birkin PR, Watson Y, White PR, Heald GJ, Dumbrell HA, Culver RL and Richards SD. The Hurst Spit experiment: The characterization of bubbles in the surf zone using multiple acoustic techniques, in *'Acoustical Oceanography', Proceedings of the Institute of Acoustics Vol. 23 Part 2, 2001,* T G Leighton, G J Heald , H Griffiths and G Griffiths, (eds.), Institute of Acoustics, (this volume), pp. 227-234.

[9] Clarke JWL and Leighton TG. A method for estimating time-dependent acoustic cross-sections of bubbles and bubble clouds prior to the steady state. *J. Acoust. Soc. Am.*,2000, **107**: 1922-1929.

[10] Keller JB, Miksis M. Bubble oscillations of large amplitude, *J. Acoust. Soc. Am.*,1980, **68**: 628-633.

[11] Herring C, Theory of the pulsation of the gas bubble produced by an underwater explosion, OSRD, Rep. No. 236 (1941).

[12] Leighton TG. The Acoustic Bubble, Academic Press, London, 1994, p. 30.

[13] Leighton TG, Ramble DG, Phelps AD, Morfey CL and Harris PP. Acoustic detection of gas bubbles in a pipe. *Acta Acustica* 1998; **84**: 801-814.

[14] Farmer DM and Vagle S. Waveguide propagation of ambient sound in the ocean-surface bubble layer. *J. Acoust. Soc. Am.* 1989; 86: 1897-1908.

[15] Leighton TG, Phelps AD and Ramble DG. Acoustic bubble sizing: from laboratory to the surf zone trials, *Acoustic Bulletin*, **21**, 1996, 5-12.

Measurement of species flux from a bubble using an acousto-electrochemical technique

P. R. Birkin[1], Y. E. Watson[1], K. L. Smith[1], T. G. Leighton[2], M. D. Simpson[2]

[1]Chemistry Department, University of Southampton, Highfield, Southampton, SO17 1BJ, UK. prb2@soton.ac.uk
[2]Institute of Sound and Vibration Research, University of Southampton, Highfield, Southampton, SO17 1BJ, UK. tgl@isvr.soton.ac.uk.

Abstract

An acousto-electrochemical technique is presented which, for the first time, offers the potential for measuring the flux of dissolved species in a liquid resulting from bubbles of a specific chosen size in the population. Laboratory trials are presented, but the device itself was damaged in the surf zone and no data was obtained from the ocean deployment. Nevertheless, the preceding laboratory tests demonstrate the viability of the technique. The device responds to perturbations of the fluid around a small electrode. Three such sources of motion must be characterised if it is to achieve the objective stated above. First, the perturbations resulting form the translatory motions of bubbles in the liquid. To obtain bubble radius resolution in the measurement of mass flux, however, it is necessary to apply to driving ('pump') sound field. Bubbles close to resonance will, in addition to a translatory motion, impart to the liquid a component of mass flux at the pump frequency. This is detected. However to show that this is the result of bubble wall pulsation, and not some other coupling, the amplitude of the pump field is increased until the electrochemical sensor detects Faraday waves on the bubble wall. Not only does this prove the relation between mass flux to bubble wall motion, it provides a second route by which the radius-resolved component of mass flux might be identified. In these preliminary laboratory tests, electrochemical detection of these motions was achieved through the observation of current produced by the reduction of a suitable redox agent present within the liquid phase of the solution employed. Preparations were made to obtain preliminary data from the Hurst Spit 2000 surf zone trial, but the device was damaged by the environment.

1. Introduction

The significance of flux of mass, momentum and energy between the atmosphere and the oceans has been recognised for several decades. The importance of subsurface oceanic bubble populations to the mass flux is known, but quantification is not simple. The ability to measure the mass flux which results from bubbles of any chosen size within a population would greatly increase our ability to test models of the bubble-mediated flux. This paper describes for the first time a technique which, after further development, would be capable of providing this measurement.

The principle of the technique is as follows. Motion within a liquid will distort the diffusion boundary layer about an electrode, and so give rise to an electrical signal which can be use to quantify the molar amount of that species detected by the electrode. Whilst many such processes (e.g. turbulence) can give rise to such time-varying signals, so too can the motion of nearby bubbles. However it is not the translation of such bubbles that is of primary interest. This is because the electrochemical effect of bubble 'fly-by' is relatively insensitive to the bubble size. Of more importance is the fluid motion caused by acoustically-generated motion of a bubble wall. Hence if the region around an electrode is insonified by a single ('pump') frequency, then the pulsation of near-resonant bubbles in the proximity of the electrode will give rise to a component of the time-varying electrical signal which is at the pump frequency. This can then be related to the flux of that species which results from those only those bubbles that are close to resonance. By varying the pump frequency, it is possible in principle to interrogate the bubbly liquid to determine the contributions of bubbles of various sizes to the mass flux. Use of a suitable model, which incorporates the contributions to fluid motion at the pump frequency of both the resonant and off-resonant bubbles, will eventually provide a measurement, resolved for bubble radius, of the mass flux from a population of bubbles across a wide size range.

In this way, this acousto-electrochemical detection is similar to the combination frequency method [1]. Both rely on the excitation of the bubble pulsation through insonification at a 'pump' frequency. However both avoid making measurements of the effect of the bubble motion on the pump sound field, and in doing so avoid the ambiguities which the presence of, for example, large off-resonance bubbles can create [1]. Instead, they both rely on detection of some other signal which is affected by the motion of the bubble wall. In the case of the combination-frequency system, this 'other signal' is the scatter of the high frequency 'imaging' field. In the case of the acousto-electrochemical system, it is the electrochemical reactions which take place at the electrode.

Given the similarities of the two techniques, it is perhaps not unsurprising that one of the first discoveries made using the combination-frequency technique, the detection of Faraday waves on the bubble wall [2, 3], should readily be replicated using the acousto-electrochemical technique. These surface waves occur on the bubble wall with a period of twice that of

TG Leighton, GJ Heald, HD Griffiths, G Griffiths, (eds.), 'Acoustical Oceanography', Proc. Institute of Acoustics Vol. 23 Part 2, 2001.

the pump field [4, 5]. Other acoustic methods, which rely solely on the use of a pump field, are on the whole insensitive to Faraday waves, because the wavelength of the latter are several orders of magnitude smaller than the wavelength of the pump field. The detection of Faraday waves by the acousto-electrochemical technique is described for the first time in this paper.

The importance of a technique for measuring bubble-mediated mass flux, and especially one with the capability to resolve the contributions made by the bubbles of various radii, is not limited to the ocean. The mass flux resulting from the generation and motion of bubbles within industrial processes, for example the chloralkali industry, has been recognised as being important in the overall efficiency of the process. Bubbles produced in this manner are thought to affect the efficiency of the overall system. In many instances the production of bubbles reduces the overall efficiency of the electrochemical system. However, electrochemically generated bubbles are also considered to enhance the transfer of material from the bulk phase of the solution within the cell to the electrode itself. Understandably, considering the scale of these industrial processes the study of bubble population within the cell is extremely important. The motion of electrochemically generated bubbles during their generation and subsequent release from the electrode has been studied intensively to understand the contribution of these processes to the mass transport of material to the electrode surface. In order to understand the mechanisms responsible for the enhancement in mass transfer to the electrodes a number of electrochemical investigations have been reported. Among these studies the work by Tobias *et al.* [8] is noteworthy. These authors used electrochemical generation and electrochemical detection of the effects of bubble release and motion to assess the various aspects of the factors contribution to mass transfer of material to an electrode surface. In order to achieve these measurements Tobias *et al.* [8] employed an array of microelectrodes to electrochemically image the motion of individual bubbles. Microelectrodes are well suited to the study of bubble motion through a liquid. The impact of individual bubbles on the hemispherical diffusion pattern characteristic for microelectrodes of a critical dimension has been reported by a number of authors. The application of microelectrodes and electrochemical techniques enables not only the study of bubble motion but also enables the investigation of higher energy process associated with inertial cavitation. Birkin *et al.*[9] and Leighton *et al.* [10] showed that it was possible to measure the effects of individual cavitation bubbles. These examples of the industrial and environmental impact of bubble phenomena demonstrate the need to improve and quantify the effects of bubbles on both natural and manmade processes.

In this paper, we report here for the first time the development of the acousto-electrochemical technique for the detection of bubble-mediated mass flux in liquids. Since the technique responds to the effect on the dissolved species of motions of the bubble wall, three sources of signal must be characterised if it is to achieve the objective stated above. First, the perturbations resulting form the translatory motions of bubbles in the liquid. These are examined in Sections 2.1 and 3.1, in the so-called 'fly-by' tests. However to obtain bubble radius resolution in the measurement of mass flux, it is necessary to introduce a second factor, through the application of a 'pump' sound field which will drive bubbles into pulsation. Bubbles close to resonance will, in addition to a translatory motion, impart to the liquid a component of mass flux at the pump frequency. This oscillatory signal is detected, the bubbles being tethered to remove the translatory component in these preliminary tests (Section 3.2). The third component, also detailed in Section 3.2, of the tests exploits the generation of Faraday waves on the bubble wall. These are parametrically excited once the amplitude of wall pulsation (and hence, for a given bubble size, the amplitude of the pump field) exceeds a threshold value [7]. Faraday waves impart, to the oscillatory electrochemical signal generated by the bubble pulsation, a component at the subharmonic of the pump frequency. In these preliminary laboratory tests, electrochemical detection of these motions was achieved through the observation of current produced by the reduction of a suitable redox agent present within the liquid phase of the solution employed. Preparations were made to obtain preliminary data from the Hurst Spit 2000 surf zone trial, but the device was damaged by the extreme conditions in the field.

2. Laboratory tests: Experimental

To develop and test the technique, prior to the Hurst Spit 2000 sea trial [1], a series of three laboratory experiments were undertaken. The fly-by test employed a specific cell (Sections 2.1 and 3.1), whereas the electrochemical detection of bubble pulsation and Faraday waves used tethered bubbles (Section 3.2). Whilst these tests employed specific chemicals for ease of analysis (Section 2.3), the system was adapted to be chemically non-invasive for ocean use (Section 4).

2.1 'Fly-by' apparatus

Figure 1 shows a schematic of the fly-by experimental cell employed to detect the motion of bubbles through the cell. The cell enabled the injection of bubbles from a needle at the base. In addition a hydrophone enabled monitoring of the acoustic emission associated with bubble injection. At the top of the cell a 25 μm diameter platinum microelectrode was positioned within the path of the bubbles directly in front of a Sonitron sound source. A two-electrode arrangement was employed with a homebuilt current follower enabling both high gain (up to 1×10^8 V A^{-1}) and low noise acquisitions of the experimental data.

The observation of surface oscillations of the bubble wall was achieved by the development of a novel cell fabricated from a Mylar speaker and Perspex. This enabled sufficient room for a glass rod to support a bubble, a hydrophone, electrodes and visual observation of the phenomena occurring within the cell. Further description of this experimental set-up will be reported elsewhere.

2.2 Associated equipment

That electrochemical data, which required only low temporal resolution, was recorded on a Computer Boards DAS08/16 ADC card. The equipment was interfaced to at PC using a Quick Basic interface program. The results of experiments requiring higher temporal resolution were recorded using a Gould 465 digital oscilloscope. The data was transferred to a PC through a RS 232 cable and commercially available software. A saturated calomel electrode (SCE) or a silver wire were used as a reference electrode were stated. The sound source consisted of a Sonitron piezoelectric transducer driven by a EG&G function generator. A Bruel and Kjear 8103 hydrophone and a Bruel and Kjear 2635 charge amplifier were used to measure and amplify pressure signals where reported. All electrochemical experiments were performed in a Faraday cage in an effort to reduce electrical noise.

2.3 Chemicals

Potassium chloride, KCl (BDH, AnalR) and Ruthenium (III) hexaamine trichloride, $[Ru(NH_3)_6]Cl_3$ (Strem, 99%) were obtained commercially and used without further purification. All solutions were made up from water purified though an Elga Elect 5 water system which produced water with a resistivity above 15 MOhms cm^{1}.

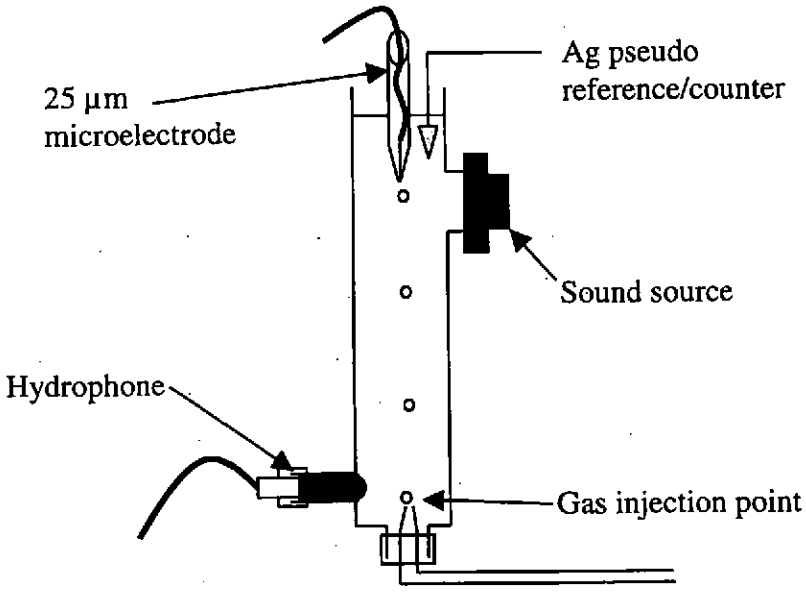

Figure 1. Schematic representation of the 'fly by' cell developed at Southampton. This cell enabled both the acoustic emission associated with bubble injection to be monitored and additional electrochemical data associated with the motion of the injected bubbles close to the electrode surface.

3. Results

3.1 'Fly-by' Experiments

If bubbles driven into oscillation were to pass within close proximity to an electrode surface, the additional mass transfer of the signal would provide a measurement of the effect on dissolved species of bubbles.

As discussed in Section 2.1, the apparatus designed to record such novel data (Figure 1) relies on the injection of bubbles through a needle placed at the base of the water column. The bubbles size is estimated from the passive emissions detected by the hydrophone upon injection (with corrections for the effect of the changing hydrostatic head as the bubble rises). After its passage up the column, the bubble approaches electrode, where the additional mass transfer as the result of bubble motion through the bulk liquid will be detected as a series of current time transients. As bubbles 'fly-by' the electrode, the diffusion layer is perturbed and a transient current spike is produced. Figure 2 shows some initial results of the apparatus showing both the hydrophone and electrochemical signals.

The hydrophone signal (solid line) detects a bubble 'signature' [11] each time one is injected. Eight bubbles are injected at regular intervals, as can be seen by the 1 s hydrophone time series of Figure 2. However the microelectrode signal responds to only one of these (at around 0.2 s). This is because the bubbles need to pass very close (of order 100 microns) to the electrode to cause a signal, making it a good local detector. The paths of the other bubbles in the figure do not result in a sufficiently close passage.

It should be noted that the fly-by cell was fitted with a transducer to supply a pump field to drive the bubbles into pulsation. Examination of that component of the electrochemical signal which is at the pump frequency, is the basis of the principle of obtaining measurements of mass flux resolved for bubble radius. However those tests were not completed prior to writing.

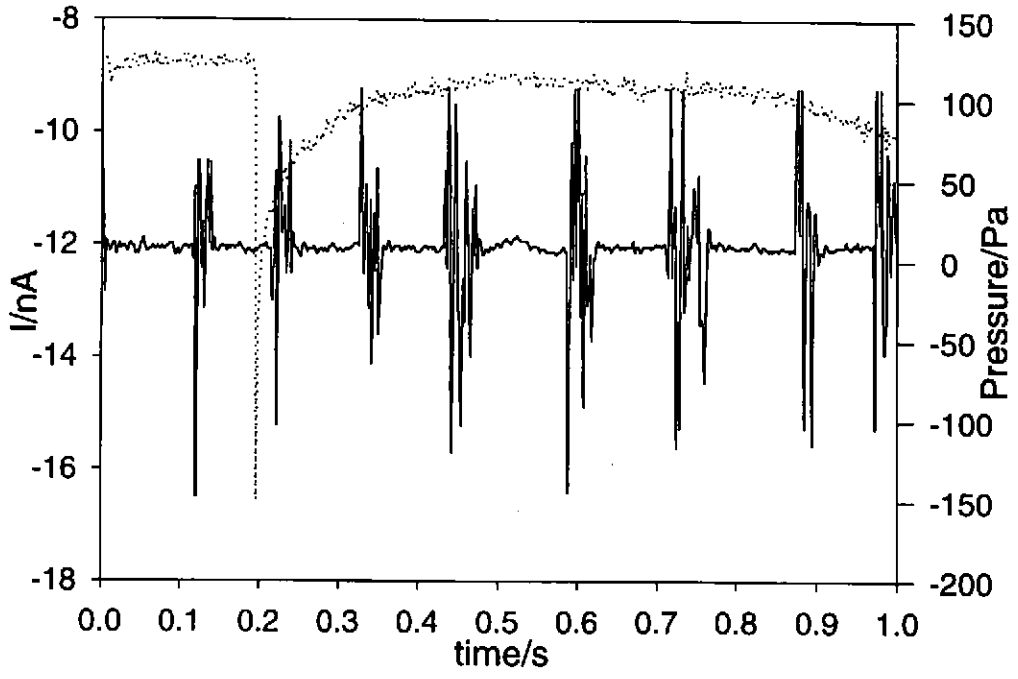

Figure 2. Plots showing the current and pressure signals recorded as a function of time. The electrochemical signal was recorded using a 25μm Pt microelectrode while the pressure was recorded using a hydrophone. The cell contained a solution of an aerobic solution of 0.1 mol dm^{-3} KCl. The potential of the electrode was held at -1.3 V versus Ag wire. The solid line represents the hydrophone response while the dotted line represents the current.

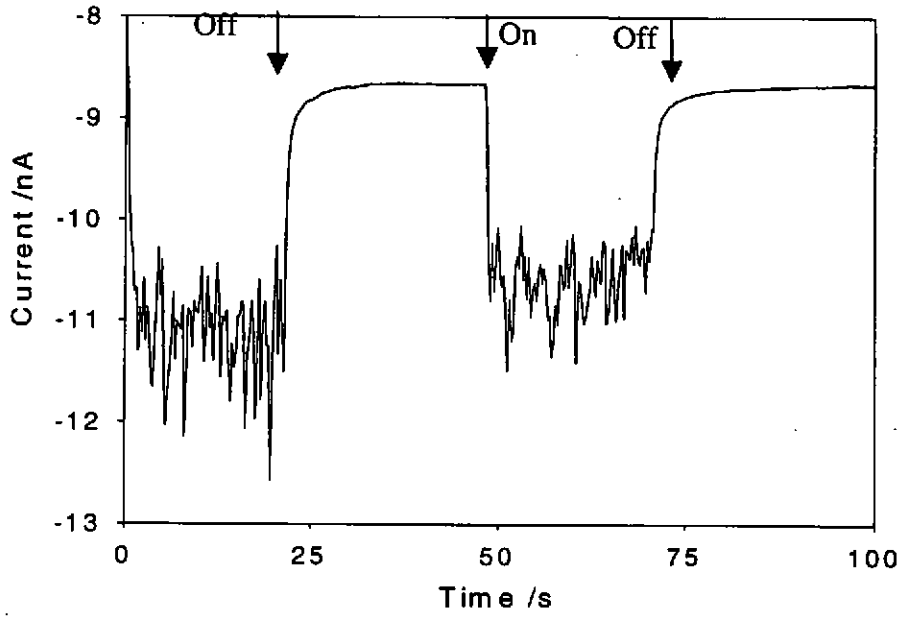

Figure 3. Current time plot obtained for an argon bubble irradiated with sound. The surface motion was detected by a 10 μm diameter Pt microelectrode. The solution contained 5 mmol dm^{-3} [Ru(NH$_3$)$_6$]Cl$_3$ in 0.1 mol dm^{-3} KCl. The solution was initially purged with argon. The potential of the electrode was maintained at –0.6 V vs. SCE. The temperature of the solution was 20-22 °C. The sound was initially on. The arrows indicate the other times during the experiment where irradiation with sound was terminated or initiated.

3.2 Electrochemical experiments in the presence of a pump field

3.2.1 Experiments with low temporal resolution

Figure 3 shows a low temporal resolution measurement of the effect of bubble oscillation on the mass transfer of a 10 μm diameter Pt microelectrode positioned within close proximity to the wall of an argon bubble. In this experiment the bubble wall held beneath a glass rod (see Figure 5), in a solution contained 5 mmol dm^{-3} [Ru(NH$_3$)$_6$]Cl$_3$ in 0.1 mol dm^{-3} KCl. The microelectrode was held at a potential sufficiently negative to reduce [Ru(NH$_3$)$_6$]$^{3+}$ ions, in this case –0.6 V vs. SCE (saturated calomel reference electrode), at a mass transfer limited steady state. In this experiment the solution had been

saturated with argon gas to remove dissolved oxygen, which is also electrochemically active at this potential. In the absence of irradiation of the bubble with sound a steady state current depicting the mass transfer characteristics of the microelectrode under normal stagnant conditions. In this case and under these conditions the steady state current (8.7 nA) implies that the diffusion coefficient of the $[Ru(NH_3)_6]^{3+}$ species was 9 x 10^{-6} cm^2 s^{-1}. This value was calculated from Equation (1):

$$i_{ss} = 4nFaDc \quad (1)$$

where i_{ss} represents the current recorded under mass transfer steady state conditions, n the number of electrons exchanged per molecule of $[Ru(NH_3)_6]^{3+}$ arriving at the surface of the electrode, F Faraday's constant, a the radius of the microelectrode, D the diffusion coefficient of the $[Ru(NH_3)_6]^{3+}$ species within the solution and c the concentration of $[Ru(NH_3)_6]^{3+}$ within the solution employed. The value of D obtained under these conditions is in agreement with the literature quoted values. In the presence of the irradiation of the bubble with sound a clear increase in the steady state current can be seen. This is attributed to the additional mass transfer as the result of convective flow of solution driven by the oscillation of the bubble wall. This noise like nature of the signal is as expected considering the time scale of the experiment and the frequency of bubble oscillation expected from a bubble irradiated at this drive frequency. The enhancement in mass transfer can be calculated from (2).

$$i = nFAk_m c \quad (2)$$

where i represents the current, k_m represents the mass transfer coefficient of the system, A the electrode area and all other terms as previously defined. In this case a mass transfer coefficient of the order of 0.029 cm s^{-1} was recorded. This is a significant number considering the already impressive mass transfer figure of 0.023 cm s^{-1} for a microelectrode in stagnant solution. This indicates that the solution around an oscillating bubble is moving relatively quickly on the electrochemical timescale employed. It was also noted that as the microelectrode was positioned further away from the surface of the bubble wall the effect of bubble oscillation showed a marked decrease.

3.2.2 Experiments with high temporal resolution

In order to temporally resolve the oscillations of the surface of the bubble wall it was necessary to employ a larger microelectrode. This was necessary particularly considering the current scale and the relatively small signal detected for the bubble wall oscillations themselves in this system. Figure 4 shows an experiment performed with a 25 µm diameter Pt microelectrode held at –0.6 V *vs.* SCE. Figure 4 contains higher time resolution data than Figure 3, again for a bubble held beneath a galss rod. It shows the current detected as the pressure amplitude of the pump field applied to an air bubble was increased. In this case the pressure close to the bubble wall was measured with a hydrophone. Though to a first approximation the hydrophone signal monitors the field which drives the bubble into pulsation, note should be made of the ability of the bubble itself to affect the signal detected at the pump frequency [6].

The solution employed in this experiment contained only 0.1 mol dm^{-3} KCl and hence only oxygen electrochemistry could be observed at the surface of the Pt microelectrode. Figure 4a shows a largely noise signal as a result of pick-up between the acoustic transducer and the high gain (1 x 10^8 V A^{-1}) electrochemical equipment used in this investigation. As the pressure was increased (see Figure 4b and Figure 4c) a strong signal associated with the visible oscillation of the bubble surface was observed. However, the frequency dependence of the signal was clearly different to the drive frequency (in this case 1.593 kHz). Figure 4b and figure 4c show a clear emergence of a signal a half the driving frequency (in this example 796 Hz). This we attribute to the excitation of Faraday waves on the surface of the bubble wall: the amplitude of the pump field required to generate this signal agrees with the amplitude theoretically required to excite Faraday waves [7]. The additional fluid motion, as a result of these surface waves, is detected as the additional mass transfer enhancement shown in Figure 3. These results show for the first time that the detection of wall motion of a stationary tethered bubble is possible using an electrochemical approach employing microelectrodes and a suitable redox system.

Figure 5 shows two images of a bubble tethered to a glass rod within the electrochemical cell employed in this study. Figure 5a shows an image of the bubble in the absence of irradiation with sound, while Figure 5b shows the same bubble driven to oscillate by an applied sound field. In this case the bubble can be clearly seen to display equatorial surface waves (which in the video sequence oscillate in the expected manner). These Faraday waves give the bubble a segmented appearance.

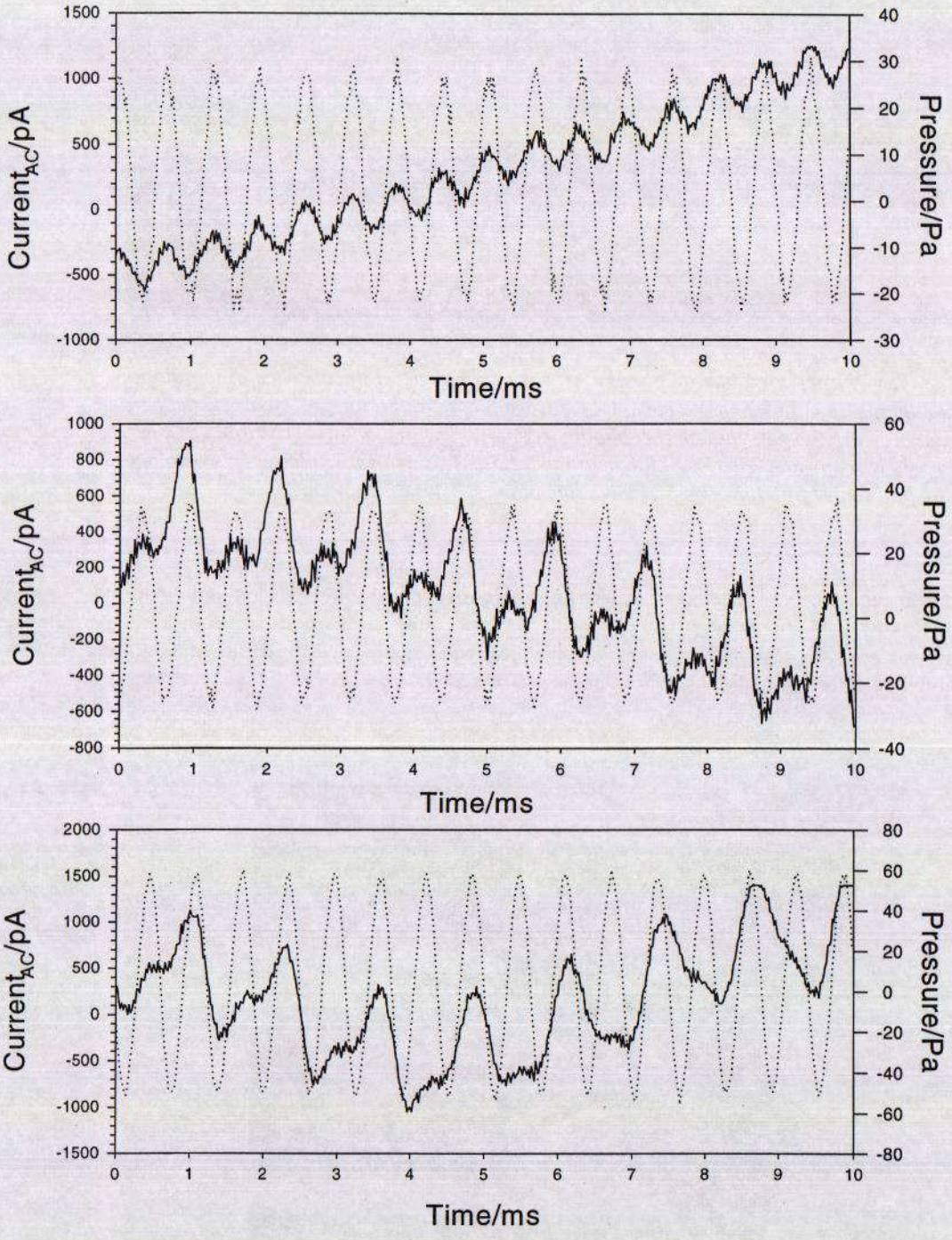

Figure 4. Plots showing the current and pressure signals recorded as a function of time as the acoustic pressure is successively increased through 'a' to 'c'. The electrochemical signal was recorded using a 25 μm Pt microelectrode while the pressure was recorded using a hydrophone. The cell contained of an aerobic solution of 0.1 mol dm^{-3} KCl. The sound irradiation frequency was 1.593 kHz. The potential of the electrode was held at -0.6 V vs. SCE. The temperature was 20-22 °C. The solid line represents the current while the dotted line the hydrophone response. Whilst the bubble clearly pulsates in sympathy with the driving field, as the amplitude of the latter is increased the generation of Faraday waves on the bubble wall is indicated by the inclusion of a component at the subharmonic of the driving frequency.

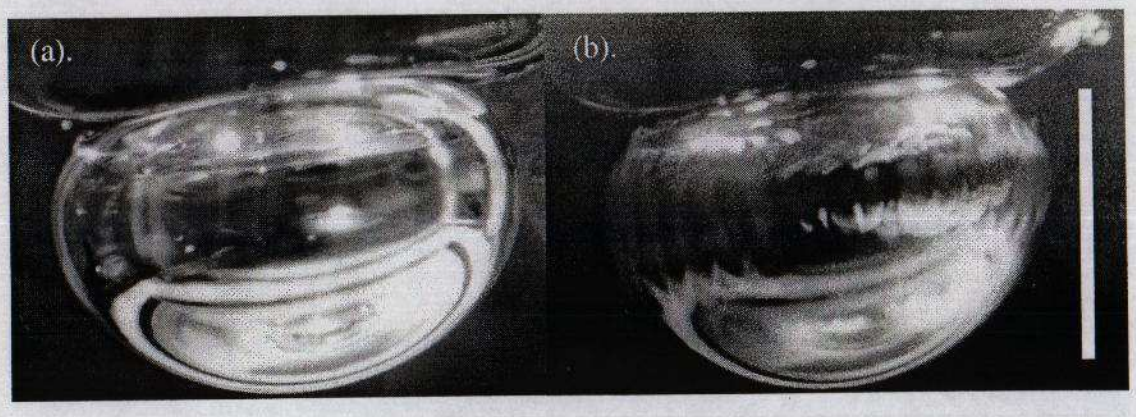

Figure 5. Image taken of a tethered bubble. Image 'a' shows a bubble in the absence of irradiation with sound while image 'b' shows the same bubble driven into oscillation by an acoustic field. Faraday waves are clearly visible about the bubble equator. The image was recorded using a Gallenkamp stereomicroscope and RICOH SLR camera and flash. An aqueous solution was employed at 20-22 °C. The white scale bar (shown as a vertical line in part 'b') is 2.5 mm long.

4. Sea Trial

The apparatus illustrated in Figure 6 was developed to determine electrochemically bubble populations at the Hurst Spit 200 sea trial [1]. It consists of a 25 μm Pt electrode set inside a copper tube, which acted as both a counter/reference electrode. The potential was held at -1.3 V vs. Ag to enhance the electrochemical signal for deployment at sea. However, the sensor was damaged by the extreme conditions present in the surf zone [1].

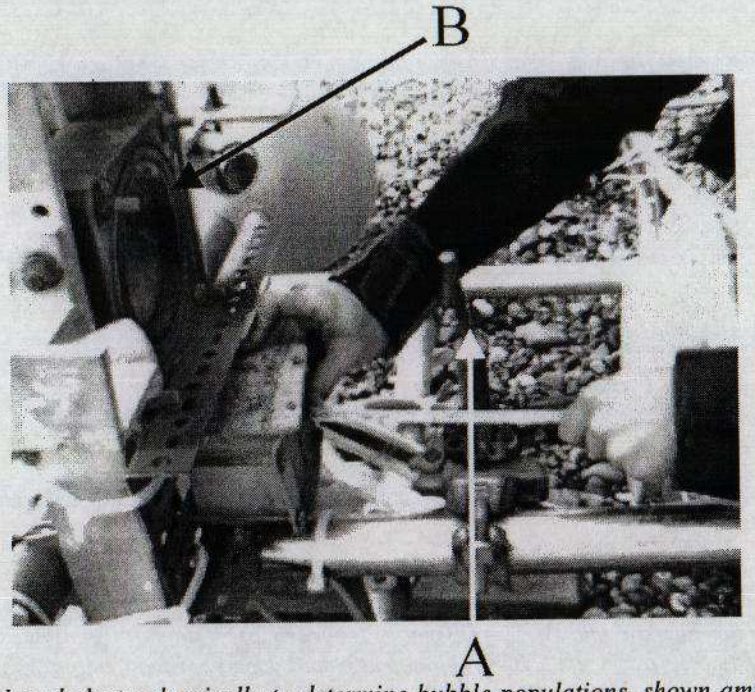

Figure 6. The sensor developed electrochemically to determine bubble populations, shown amidst in the Hurst Spit 2000 sea trial rig. The electrode tip is the white dot in centre of picture, and its shaft is labelled A. The pump frequency source (on either side of which are the combination frequency transducers) is labelled B.

5. Conclusions

An electrochemical signal resulting from the passage close to an electrode of a bubble has been reported, and the local nature of the detector illustrated. The detection of bubble oscillation as the result of acoustic irradiation of a stationary bubble has been reported for the first time. Electrochemical evidence for subharmonic motion on the surface of the bubble, associated with the well-known phenomena of Faraday waves, has been reported for the first time. Details of how to adapt this system to the ocean are given, but no ocean data was obtained because of damage. Further laboratory tests, including 'fly-by' tests in the presence of a pump field, and a bubble population covering a wide radius range, are planned prior to the next sea trial. To date only the first half of Objective (ii) from Section 3 of Leighton *et al.* [17] has been accomplished.

References

[1] Leighton TG, Meers SD, Simpson MD, Clarke JWL, Yim GT, Birkin PR, Watson Y, White PR, Heald GJ, Dumbrell HA, Culver RL and Richards SD. The Hurst Spit experiment: The characterisation of bubbles in the surf zone using multiple acoustic techniques, in *'Acoustical Oceanography', Proceedings of the Institute of Acoustics Vol. 23 Part 2, 2001,* T G Leighton, G J Heald , H Griffiths and G Griffiths, (eds.), Institute of Acoustics, (this volume), pp. 227-234.

[2] Leighton TG, Lingard RJ, Walton AJ and Field JE. Acoustic bubble sizing by the combination of subharmonic emissions with an imaging frequency. *Ultrasonics*, 1991; **29**: 319-323.

[3] Leighton TG, Lingard RJ, Walton AJ and Field JE. Bubble sizing by the nonlinear scattering of two acoustic frequencies, in *Natural Physical Sources of Underwater Sound* (Ed. B Kerman), Kluwer Academic Publishers Ltd, 1993, 453-466.

[4] Phelps AD and Leighton TG. High resolution bubble sizing through detection of the subharmonic response with a two frequency excitation technique. *Journal of the Acoustical Society of America*, 1996; **99**: 1985-1992.

[5] Phelps AD and Leighton TG. The subharmonic oscillations and combination-frequency emissions from a resonant bubble: their properties and generation mechanisms. *Acta Acustica*, 1997; **83**: 59-66.

[6] Leighton TG, Ramble DG and Phelps AD. The detection of tethered and rising bubbles using multiple acoustic techniques. *Journal of the Acoustical Society of America*, 1997; **101**: 2626-2635.

[7] Ramble DG, Phelps AD and Leighton TG. On the relation between surface waves on a bubble and the subharmonic combination-frequency emission. *Acta Acustica*, 1998; **84**: 986-988

[8] Whitney GM and Tobias CW. Mass-transfer effects of bubble streams rising near vertical electrodes. *AIChE Journal*, 1988; **34**: 1988.

[9] Birkin PR, O'Conner R, Rapple C and Silva Martinez S. Electrochemical measurement of erosion from individual cavitation events generated from continuous ultrasound. *J. Chem. Soc., Faraday Trans.*, 1998; **94**: 3365-3371.

[10] Leighton TG, Cox BT, Birkin PR and Bayliss T. The Rayleigh-like collapse of a conical bubble: Measurements of menicus, liquid pressure and electrochemistry. *Proceedings of the 137th regular Meeting of the Acoustical Society of America and the 2nd Convention of the European Acoustics Association (Forum Acusticum 99, integrating the 25th German Acoustics DAGA Conference).* March 1999, Paper 3APAB_ 1.

[11] Yim GT, White PR, and Leighton TG, Estimation of the time, location and natural frequency of entrained bubbles, through identification of individual bubble signatures in a severely overlapping, noisy surf zone environment, in *'Acoustical Oceanography', Proceedings of the Institute of Acoustics Vol. 23 Part 2, 2001,* T G Leighton, G J Heald, H Griffiths and G Griffiths, (eds.), Institute of Acoustics, (this volume), pp. 250-256.